JPE 16-2-36

http://dx.doi.org/10.6113/JPE.2016.16.2.778
ISSN(Print): 1598-2092 / ISSN(Online): 2093-4718

An Excess Carrier Lifetime Extraction Method for Physics-based IGBT Models

Guicui Fu* and Peng Xue†

*, †School of Reliability and System Engineering, Beihang University, Beijing, China

Abstract

An excess carrier lifetime extraction method is derived for physics-based insulated gate bipolar transistor (IGBT) models with consideration of the latest development in IGBT modeling. On the basis of the 2D mixed-mode Sentaurus simulation, the clamp turn-off test is simulated to obtain the tail current. The proposed excess carrier lifetime extraction method is then performed using the simulated data. The comparison between the extracted results and actual lifetime directly obtained from the numerical device model precisely demonstrates the accuracy of the proposed method.

Key words: Excess carrier lifetime, IGBT, Parameter extraction, 2D Sentaurus simulation

I. INTRODUCTION

In recent years, the characterization and modeling of insulated gate bipolar transistors (IGBTs) have been greatly improved [1]–[6]. In particular, the physics-based models for non-punch-through (NPT), punch-through (PT), and field-stop (FS) IGBTs have become increasingly accurate. However, precise IGBT models are not enough. Thus, including a parameter extraction method that can accurately extract the parameters needed for the models is necessary.

Excess carrier lifetime is one of the most important parameters for physics-based IGBT models, which characterize the tail current during the turn-off transient and on-state voltage drop. Although many works have explored lifetime extraction [7]-[19], most of them use the extraction theory cited in [7] to extract excess carrier lifetime for NPT IGBT models, as well as the extraction theory cited in [17] to extract excess carrier lifetime for PT or FS IGBT models. Since the significant development of IGBT transient modeling theory, especially the availability of the newly proposed expression for the transient dynamics of excess carrier distribution in the N-base [4] and the improved understanding of the transient modeling of FS layers [5], extraction methods should be modified to meet the latest developments. Moreover, many existing studies validated their extraction methods by comparing the experimental and simulated characteristics of IGBTs at static and transient states. Such validation approach is not enough. As simulation accuracy depends on many factors, the accuracy of simulation results cannot guarantee the accuracy of extraction methods.

In the present study, an excess carrier lifetime extraction method for physics-based IGBT models is is proposed on the basis of the latest development in IGBT modeling theory [4], [5]. The Sentaurus simulation is used to validate the proposed method. In the validation, the Sentaurus 2D mixed-mode simulation is used to simulate the clamp voltage turn-off test. The proposed extraction method is implemented with the simulation data. Finally, the comparison between the extracted results and the actual lifetime obtained from the numerical device model validates the proposed method.

II. EXCESS CARRIER LIFETIME EXTRACTION METHOD

The excess carrier lifetime is extracted by the tail current at a constant voltage supply, which is obtained from the clamp voltage turn-off test. For NPT IGBTs, the extraction of N-base lifetime τ_L is independent of clamp voltage. For PT and FS IGBTs, a low clamp voltage extraction is needed to acquire the N-base lifetime τ_L, and a high clamp voltage extraction is necessary to obtain the buffer layer lifetime τ_H.

A. Extraction of τ_L for NPT IGBT Models

Manuscript received Jun. 21, 2015; accepted Nov. 11, 2015
Recommended for publication by Associate Editor Jee-Hoon Jung.
†Corresponding Author: demosupen@buaa.edu.cn
Tel: +86-8233-9623, Fax: +86-8233-9519, Beihang University
*School of Reliability and System Engineering, Beihang University, China

According to Hefner's IGBT modeling theory [7], during the turn-off transient state, the base charge decay rate is

$$\frac{dQ_L}{dt} = -\frac{Q_L}{\tau_L} - I_{n0} \quad (1)$$

where Q_L is the excess carrier charge in the N-base, τ_L is the excess carrier lifetime in the N-base, and I_{n0} is the electron current injected into the emitter.

Q_L in (1) is expressed as [7]

$$Q_L = I_T \frac{W_L^2}{4D_P} \quad (2)$$

where W_L is the undepleted N-base width. D_P is the hole diffusivity in the N-base, and I_T is the total current.

I_{n0} in (1) is expressed as [7]

$$I_{n0} = \frac{I_{sne} P_0^2}{n_i^2} \quad (3)$$

where n_i is the intrinsic carrier concentration, I_{sne} is the emitter electron saturation current, and P_0 is the excess carrier concentration at the emitter edge of the N-base.

At the turn-off transient state, if the anode voltage rise time is prolonged, then few electrons can arrive to the P emitter to provide the electrons needed for recombination. The local electrons and holes thereby have to recombine, which results in the decrement of P_0. As I_{n0} is proportional to the square of P_0, I_{n0} dramatically drops when P_0 decreases. Therefore, in prolonging the anode voltage rise time, I_{n0} in (1) can be neglected. Substituting (2) into (1) yields

$$\tau_L = -\left[\frac{dlnI_T}{dt}\right]^{-1} \quad (4)$$

The current decay rate ($-[dlnI_T / dt]^{-1}$) decreases at a low current because the N-base leaves a high-level injection condition and the low-level lifetime is shorter than the high-level lifetime. At a high current, the current decay rate also decreases because the increased rate of emitter electron current injection [7]. In the range in which the current decay rate is at its maximum, the N-base is in a high-level injection state, and the electron current injection is negligible, (4) is valid. τ_L is equal to the maximum value of the current decay rate.

B. Extraction of τ_L and τ_H for PT IGBT Models

In a PT IGBT, the N-base is in a high-level injection condition. Therefore, the whole current transmission equation takes the form of the following bipolar transport equation [20]:

$$I_{pL} = \frac{I_T}{1+b_L} - qAD_L \frac{d(\delta p)}{dx} \quad (5)$$

where $D_L = 2D_{NL}D_{PL}/(D_{NL}+D_{PL})$. D_{NL} and D_{PL} are the electron and hole diffusivities in the N-base, respectively. $b_L = \mu_{NL}/\mu_{PL}$. μ_{NL} and μ_{PL} are the electron and hole mobilities in the N-base, respectively. δp is the excess hole concentration, and A is the device active area.

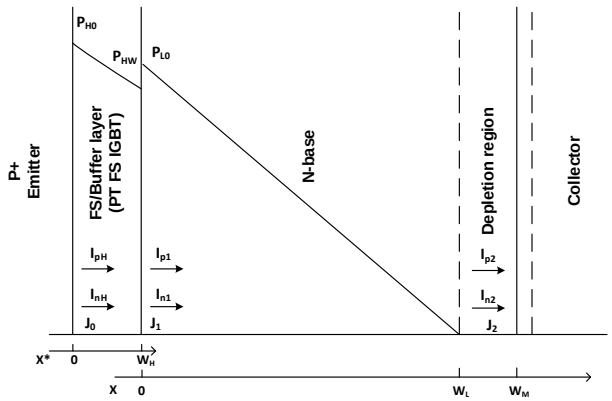

Fig. 1. Coordinate diagram for the PT and FS IGBTs.

At the turn-off transient state, the N-base excess hole distribution is [4], [5]

$$\delta p(x,t) = P_{L0}\left[1-\frac{x}{W_L}\right] - \frac{P_{L0}}{W_L D_L}\frac{dW_L}{dt}\left[\frac{x^2}{2} - \frac{W_L x}{6} - \frac{x^3}{3W_L}\right] + P_{L0}\left[\frac{x^2}{2L_L^2} - \frac{x^3}{6W_L L_L^2} - \frac{xW_L}{3L_L^2}\right] \quad (6)$$

where W_L is the width of the undepleted N-base, P_{L0} is the excess carrier concentration at $x=0$ (Fig. 1), and L_L is the base diffusion length $L_L = \sqrt{D_L \tau_L}$.

In the clamp voltage turn-off test, after the anode voltage reaches the clamp voltage, the anode voltage remains constant. Therefore, dW_L/dt in (6) is zero. By combining (5) and (6) while neglecting the second term of (6), we can obtain the base hole currents I_{p1} and I_{p2} in Fig. 1.

$$I_{p1} = I_{pL}(x=0) = \frac{I_T}{1+b_L} + \frac{Q_L}{\tau_{Ab}} + \frac{2Q_L}{3\tau_L} \quad (7)$$

$$I_{p2} = I_{pL}(x=W_L) = \frac{I_T}{1+b_L} + \frac{Q_L}{\tau_{Ab}} - \frac{Q_L}{3\tau_L} \quad (8)$$

where τ_{Ab} is the ambipolar base transit time $\tau_{Ab} = W_L^2/2D_L$. The N-base excess charge is $Q_L = qP_{L0}W_L/2$.

In the PT buffer layer, the low-level injection is assumed, and the hole current I_{pH} is [20]

$$I_{pH} = \frac{qAD_{PH}}{W_H}(P_{H0} - P_{HW}) = \frac{Q_H}{\tau_{Hb}} - \frac{4}{\tau_{Hb}}\frac{W_H}{W_L}\frac{N_L}{N_H}\frac{Q_L^2}{Q_B} \quad (9)$$

where W_H is the buffer layer width. N_H is the buffer layer

doping concentration. P_{H0} and P_{HW} are the excess carrier concentrations at $x^*=0$ and $x^*=W_H$, respectively. Q_H is the excess charge in the buffer layer, that is, $Q_H = qAW_H(P_{H0}+P_{HW})/2$. Q_B is the base charge, that is, $Q_B = qAW_L N_L$. τ_{Hb} is the buffer layer base transit time, that is, $\tau_{Hb} = W_H^2 / 2D_{PH}$.

Note that $N_L << N_H$ and that the second term on the right side of (9) is much smaller than the first term [5]. By equating (7) and (9) while neglecting the second term of (9), we can express the base charge Q_L as

$$Q_L = \frac{Q_T - \frac{I_T}{1+b_L}\tau_{Hb}}{1+\frac{\tau_{Hb}}{\tau_{Ab}}+\frac{2\tau_{Hb}}{3\tau_L}} \tag{10}$$

where Q_T is the total excess charge in the N-base and buffer layer. $Q_T = Q_H + Q_L$. By substituting (10) into (8), the hole current I_{p2} at $x=W_L$, which is now the total current, is given by

$$I_T = \frac{Q_T\left(\frac{1}{\tau_{Ab}}-\frac{1}{3\tau_L}\right)}{\frac{\tau_{Hb}}{\tau_{Ab}}+\frac{b_L}{1+b_L}+\frac{(2b_L-1)\tau_{Hb}}{3(1+b_L)\tau_L}} \tag{11}$$

The total charge decay rate is [20]

$$\frac{dQ_T}{dt} = -\left(\frac{W_L^2}{4D_{PL}\tau_L}+\frac{W_H^2}{2D_{PH}\tau_H}+\frac{W_H N_H I_{sne}}{D_{PH}qn_i^2 A}\right)I_T - \left(\frac{qAW_H}{\tau_H N_H}+\frac{I_{sne}}{n_i^2}\right)\left(\frac{W_L}{2qAD_{PL}}\right)^2 I_T^2 \tag{12}$$

where τ_H is the excess carrier lifetime in a high-doped buffer layer.

For the high clamp voltage extraction $W_L \approx 0$, (11) is simplified as

$$I_T = \frac{Q_T}{\tau_{Hb}} \tag{13}$$

Substituting (13) into (12) with $W_L = 0$ yields (14).

$$\frac{dln(I_T)}{dt} = -\left(\frac{1}{\tau_H}+\frac{2N_H I_{sne}}{qAW_H n_i^2}\right) \tag{14}$$

The first term on the right side of (14) corresponds to the excess charge recombination in the buffer layer, whereas the second term denotes the emitter electron current injection. The excess charge recombination rate in the buffer layer is much larger than the electron injection rate because τ_H is very short. If the second term on the right side of (14) can be neglected, then (15) is obtained.

$$\tau_H = -\left[\frac{dlnI_T}{dt}\right]^{-1} \tag{15}$$

At a high current, the buffer layer leaves the low-level injection condition. The current decay rate thereby increases because the high-level lifetime is longer than the low-level lifetime. At a low current, the excess charge in the buffer layer is almost exhausted, and the current decay is dominated by the electron current injection. The current decay rate increases because of the decreased rate of emitter electron current injection. In the minimum current range, in which the buffer layer is in a low-level injection condition and the electron current injection is negligible, (15) is valid. τ_H is equal to the minimum value of the current decay rate.

For the low clamp voltage extraction, $\tau_{Ab} \ll \tau_L$ is observed, and (11) is simplified as

$$I_T = \frac{\frac{Q_T}{\tau_{Ab}}}{\frac{\tau_{Hb}}{\tau_{Ab}}+\frac{b_L}{1+b_L}+\frac{(2b_L-1)\tau_{Hb}}{3(1+b_L)\tau_L}} \tag{16}$$

The anode voltage rise time is prolonged. Few electrons can reach the J_0 junction to provide the electrons needed for recombination. Therefore, the local electrons and holes are recombined, and P_{H0} is decreased. The excess carrier recombination rate is very large because the excess carrier lifetime in the buffer layer is very short. Thus, P_{H0} greatly decreases as a result of the recombination. In the PT IGBT, the electron current injected into the emitter is [17]

$$I_{nH} = \frac{I_{sne}P_{H0}N_H}{n_i^2} \tag{17}$$

The electron current I_{nH} injected into the emitter is thereby negligible because of the significant decrement of P_{H0}.

The anode voltage rise time is prolonged to eliminate electron current injection. The terms containing I_{sne} in (12) correspond to the electron current injection. By neglecting the terms containing I_{sne} in (12), substituting (16) into (12) yields

$$\frac{dln(I_T)}{dt} = -\frac{1}{\tau_{eff}^p}\left(1+\frac{I_T}{I_k^p}\right) \tag{18}$$

where

$$\frac{1}{\tau_{eff}^p} = \frac{\frac{1}{\tau_{Ab}}\left(\frac{W_L^2}{4D_{PL}\tau_L}+\frac{W_H^2}{2D_{PH}\tau_H}\right)}{\frac{\tau_{Hb}}{\tau_{Ab}}+\frac{b_L}{1+b_L}+\frac{(2b_L-1)\tau_{Hb}}{3(1+b_L)\tau_L}} \tag{19}$$

and

$$\frac{1}{I_k^p\tau_{eff}^p} = \frac{\frac{1}{\tau_{Ab}}\frac{qAW_H}{\tau_H N_H}\left(\frac{W_L}{2qAD_L}\right)^2}{\frac{\tau_{Hb}}{\tau_{Ab}}+\frac{b_L}{1+b_L}+\frac{(2b_L-1)\tau_{Hb}}{3(1+b_L)\tau_L}} \tag{20}$$

According to the discussion on (4), (18) is only validated in the range in which the current decay rate is at its maximum.

In this range, I_T is much smaller than I_k^p. Therefore, τ_{eff}^p is approximately equal to the maximum current decay rate, which can be used in (19) to calculate τ_L.

C. Extraction of τ_L and τ_H for FS IGBT Models

In the FS IGBT, the N-base is also in a high-level injection condition; hence, equations (5)–(8) are still valid. However, unlike the PT buffer layer, the FS layer is in a high-level injection condition [5]; therefore, (9) should be modified as

$$I_{pH} = \frac{I_T}{1+b_H} + \frac{qAD_{PH}}{W_H}(P_{H0} - P_{HW}) = \frac{I_T}{1+b_H} + \frac{Q_H}{\tau_{Hb}} - \frac{4}{\tau_{Hb}}\frac{W_H}{W_L}\frac{N_L}{N_H}\frac{Q_L^2}{Q_B} \quad (21)$$

The doping concentration in the FS layer is about $1\times10^{15}cm^{-3} - 1\times10^{16}cm^{-3}$; thus, $b_H \approx b_L$. As $N_L << N_H$, the third term of (21) can be neglected [5]. By equating (7) and (21), the base charge Q_L is expressed as

$$Q_L = \frac{Q_T}{1+\frac{\tau_{Hb}}{\tau_{Ab}}+\frac{2\tau_{Hb}}{3\tau_L}} \quad (22)$$

By substituting (22) into (8), the collector current, which is now the total current, is given by

$$I_T = \frac{\frac{1+b_L}{b_L}\left(\frac{Q_T}{\tau_{Ab}} - \frac{Q_T}{3\tau_L}\right)}{1+\frac{\tau_{Hb}}{\tau_{Ab}}+\frac{2\tau_{Hb}}{3\tau_L}} \quad (23)$$

For the high clamp voltage extraction, (23) is simplified as follows because $W_L \approx 0$:

$$I_T = \frac{1+b_L}{b_L}\frac{Q_T}{\tau_{Hb}} \quad (24)$$

According to the discussion in (14), the emitter electron current injection is negligible. By eliminating the terms containing I_{sne} in (12), substituting (24) into (12) with $W_L = 0$ yields

$$\tau_H = -\frac{1+b_L}{b_L}\left[\frac{dlnI_T}{dt}\right]^{-1} \quad (25)$$

The current decay rate decreases at a high current because of the increased rate of electron injection into the emitter. At a low current, the current decay rate also decreases because the FS layer leaves a high-level injection condition. Therefore, in the maximum current range, in which the FS layer is in a high-level injection condition and the electron current injection is negligible, (25) is valid. The maximum current decay rate can be used in (25) to calculate τ_H.

$$I_T = \frac{\frac{(1+b_L)}{b_L}\frac{Q_T}{\tau_{Ab}}}{1+\frac{\tau_{Hb}}{\tau_{Ab}}+\frac{2\tau_{Hb}}{3\tau_L}} \quad (26)$$

For the low clamp voltage extraction, $\tau_{Ab} \ll \tau_L$; hence,

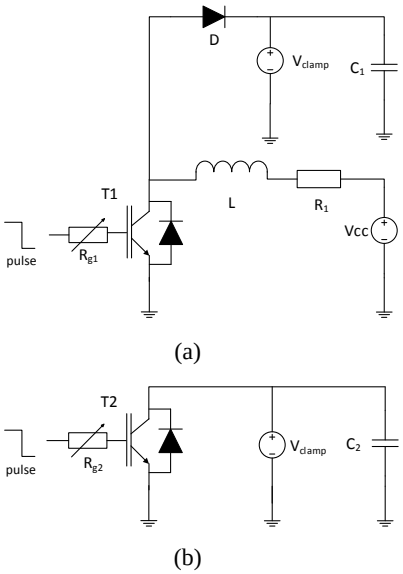

Fig. 2. Test circuit used for excess lifetime extraction. (a) Circuit used to extract τ_L for NPT IGBT and τ_H for FS or PT IGBT. (b) Circuit used to extract τ_L for the FS or PT IGBT.

(23) is simplified as

$$\frac{dln(I_T)}{dt} = -\frac{1}{\tau_{eff}^f}\left(1+\frac{I_T}{I_k^f}\right) \quad (27)$$

where

$$\frac{1}{\tau_{eff}^f} = \frac{\frac{1+b_L}{b_L}\frac{1}{\tau_{Ab}}\left(\frac{W_L^2}{4D_P\tau_L}+\frac{W_H^2}{2D_P\tau_H}\right)}{1+\frac{\tau_{Hb}}{\tau_{Ab}}+\frac{2\tau_{Hb}}{3\tau_L}} \quad (28)$$

and

$$\frac{1}{I_k^f\tau_{eff}^f} = \frac{\frac{1+b_L}{b_L}\frac{1}{\tau_{Ab}}\frac{qAW_H}{\tau_H N_H}\left(\frac{W_L}{2qAD_{PL}}\right)^2}{1+\frac{\tau_{Hb}}{\tau_{Ab}}+\frac{2\tau_{Hb}}{3\tau_L}} \quad (29)$$

According to the discussion on (4), (27) is also valid in the range in which the current decay rate is at its maximum. In this range, I_T is much smaller than I_k^f. Therefore, τ_{eff}^f is equal to the maximum current decay rate, which can be used in (28) to calculate τ_L.

III. Numerical Simulation

To validate the proposed extraction method, the tail current is obtained with the 2D Sentaurus numerical simulation. In the simulation, the test circuits (Fig. 2) are used to simulate the clamp voltage turn-off test. Through the Sentaurus mixed-mode simulation, all the diodes, resistors, and inductors used in the test are implemented with built-in Sentaurus compact models. The NPT, PT, and FS IGBTs

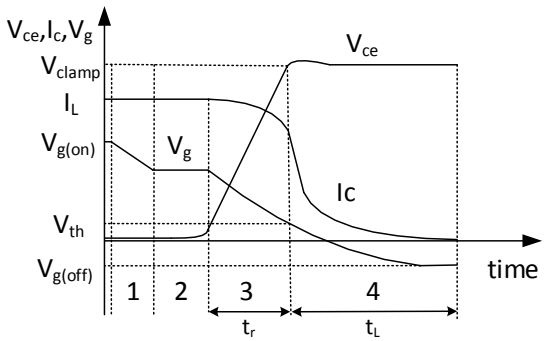

Fig. 3. Typical waveforms of IGBT turn-off process.

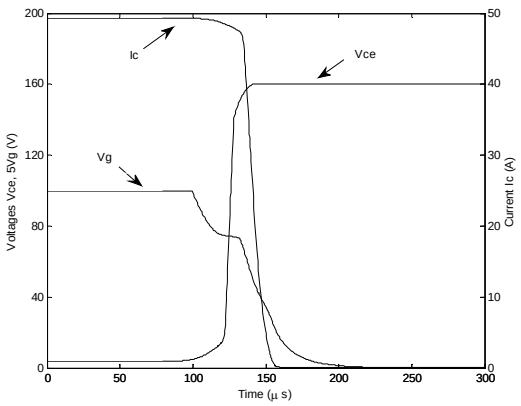

Fig. 4. Turn-off waveforms of the simulated clamp voltage of the NPT IGBT using $R_g = 5k\Omega$ at 150 V/50 A.

under testing are implemented with 2D numerical device models. Table 2 shows the parameters used in the 2D numerical device models.

According to the mixed-mode simulation, the turn-off waveforms of the clamp voltage can be obtained. The typical and simulated turn-off waveforms are shown in Figs. 3 and 4, respectively. Fig. 3 shows that the turn-off transient condition of the IGBT can be divided into four phases. In phase 1, the gate-side capacitance discharges, and the gate voltage Vg decreases accordingly. In phase 2, as a result of the Miller effect, Vg remains approximately constant. Vce starts to rise slowly while the collector current Ic remains unchanged. As the collector-emitter voltage Vce increases to approximately 10 V, phase 3 begins. Vce begins to increase rapidly toward Vdc. In this phase, the collector-emitter depletion capacitance begins to charge. The charging current greatly compensates for the collector current reduction because of the shrinking of the MOS-side electron current. The collector current Ic then undergoes a slow decrease. Once Vce reaches the Vclamp, phase 4 begins. The diode begins to conduct, and the collector current of the IGBT starts to transfer into the diode. Given that Vge is under the threshold voltage Vth, the MOS-side electron current and the associated hole drift current are removed. This effect results in an initial rapid decline of the collector current Ic. The collector current Ic then continues to decline because of the remaining excess carrier recombination in the N-base and buffer layer.

TABLE I
2D NUMERICAL DEVICE MODEL PARAMETER LIST

Parameter	NPT IGBT	PT IGBT	FS IGBT
N-base doping concentration (cm^{-3})	5×10^{13}	5×10^{13}	5×10^{13}
N-base width (μ m)	140	70	70
Cell pitch width (μ m)	10	10	10
Trench gate depth (μ m)	8	8	8
Trench gate width (μ m)	3	3	3
PT buffer layer/FS layer width (μ m)	-	6	4
PT buffer layer/FS layer doping concentration (cm^{-3})	-	1×10^{17}	5×10^{15}
P emitter width (μ m)	4	10	4
P emitter doping concentration(cm^{-3})	5×10^{16}	5×10^{18}	1×10^{17}

As shown in Fig. 3, the duration of phase 3 and that of phase 4 are defined as t_r and t_L, respectively. During t_L, the excess carrier in the N-base and buffer layer undergo slow recombination. The current decay rate during t_L can thus be used to extract the excess carrier lifetime. t_r is the anode voltage rise time. To eliminate the excess carrier concentration P_0 at the emitter edge of the N-base, t_r should be long enough. In the range in which the extracted carrier lifetime is independent of t_r, the extracted results are equal to the real carrier lifetime.

IV. EXTRACTION METHOD VALIDATION

On the basis of the simulated tail current, the proposed lifetime extraction method is performed to extract the excess carrier lifetime. The extraction method is directly validated by comparing its excess carrier lifetime with the actual excess carrier lifetime obtained from the 2D numerical device model.

A. Excess lifetime extraction for NPT IGBT models

The circuit in Fig. 2a is used to simulate the turn-off test. In the circuit, the clamp voltage V_{clamp} is 150 V, the inductor L is 2 mH, the source voltage V_{cc} is 500 V, the capacitance C_1 is 50 mF, the load resistor R_1 is 5 Ω, and the gate resistor R_{g1} is varied to change the anode voltage rise time.

The turn-off tests are simulated with six different anode voltage rise times at 150 V/50 A. On the basis of the simulated tail current, the current decay rate is calculated

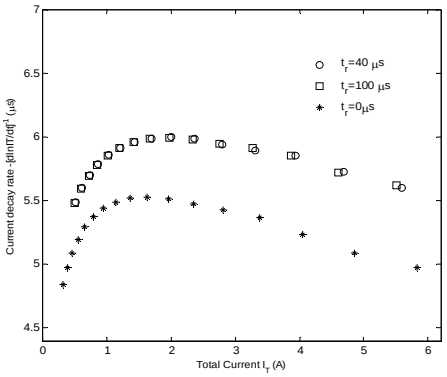

Fig. 5. Current decay rate versus total current for NPT IGBT.

with (4), as shown in Fig. 5. In the range in which the maximum current decay rate is independent of the anode voltage rise time, τ_L is extracted to be 6.01 μs. The actual lifetime τ_L obtained from the NPT IGBT device model is 6.2 μs, which is very close to the extracted value.

B. Excess Lifetime Extraction for PT IGBT Models

For the high clamp voltage extraction of the PT IGBT, the test circuit in Fig. 2a is used to extract τ_H. In the circuit, the inductor L is 2 mH, the gate resistor R_{g1} is set to zero, the voltage of V_{cc} is 600 V, the capacitance C_1 is 50 mF, the load resistor R_1 is 5 Ω, and the clamp voltage V_{clamp} ranges from 300 V to 550 V. This extraction is performed to verify that the proposed method can provide a reasonable extraction result at different clamp voltages.

The turn-off test is simulated at 50 A. The current decay rate is then calculated with (15). τ_H is extracted by finding the minimum value of the current decay rate. Fig. 6 shows the extracted τ_H at different clamp voltages.

For the low clamp voltage extraction, the test circuit in Fig. 2b is used to extract τ_L. In the circuit, the clamp voltage V_{clamp} is 5 V, the capacitance C_2 is 100 mF, and the gate resistor R_{g2} is varied to change the anode voltage rise time.

The turn-off test is carried out at 5 V/50 A. On the basis of the simulated tail current, the current decay rate is calculated, as shown in Fig. 7. In the range in which the maximum current decay rate is approximately independent of the anode voltage rise time, τ_{eff}^{p} is extracted to be 4.26 μs. By substituting the extracted τ_{eff}^{p} into (19), τ_L is calculated to be $6.23\mu s$.

The actual τ_L and τ_H of the PT IGBT device model are $6.3\mu s$ and $28ns$, respectively. The extracted τ_L and τ_H show great accuracy.

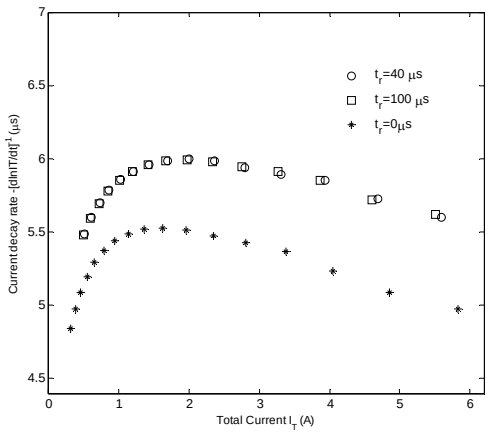

Fig. 6. Extracted τ_H versus clamp voltage for PT IGBT.

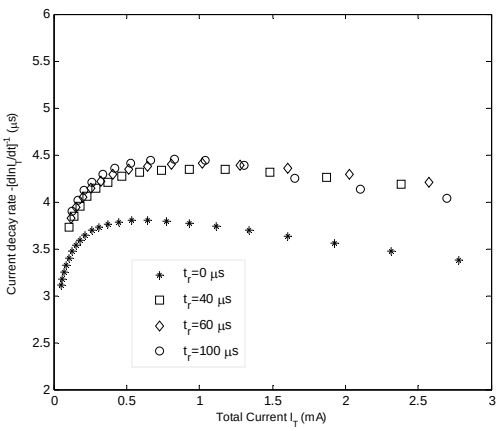

Fig. 7. Current decay rate versus total current for PT IGBT.

C. Extraction for FS IGBT models

For the high clamp voltage extraction of the FS IGBT, the circuit in Fig. 2(a) is used to extract τ_H. All parameters in the circuit are the same as those used for the high clamp voltage extraction of the PT IGBT. The maximum current decay rate is determined, and τ_H is then extracted with (25). The extracted τ_H is plotted versus various clamped voltages in Fig. 8.

For the low clamp voltage extraction, the turn-off test is simulated at 5 V/50 A with the circuit in Fig. 2b. In the circuit, the capacitance C_2 is 100 mF. The gate resistor R_{g2} is varied to change the anode voltage rise time. On the basis of the simulated tail current, the current decay rate is extracted (Fig. 9). In the range in which the maximum current decay rate is independent of the anode voltage rise time, τ_{eff}^{f} is equal to the maximum current decay rate ($4.35\mu s$). By substituting τ_{eff}^{f} to (28), τ_L is extracted to be $5.6\mu s$.

The actual τ_L and τ_H obtained from the FS IGB T

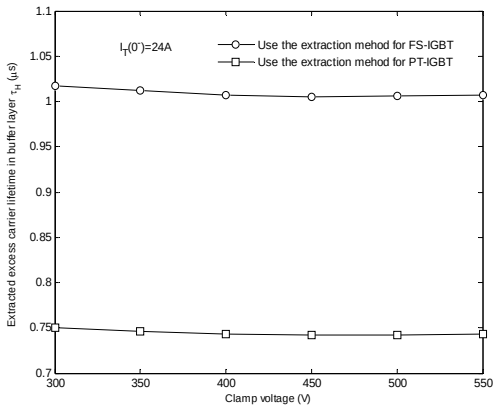

Fig. 8. Extracted τ_H versus clamp voltage for FS IGBT.

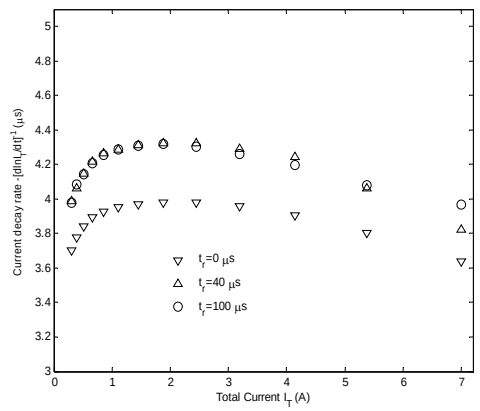

Fig. 9. Current decay rate versus total current for FS IGBT.

device model are $6\mu s$ and $1\mu s$, respectively. The extracted τ_L and τ_H are very close to the actual value.

The extracted τ_H is greatly overestimated when the extraction method for the PT IGBT is used to extract the lifetime, as shown in Fig. 9. This overestimation is caused by the FS layer being in a high-level injection condition [5] and the PT buffer layer being in a low-level injection condition; moreover, the lifetime of the high-level injection is longer than that of the low-level injection.

V. CONCLUSION

A novel excess carrier lifetime extraction method is proposed in this work. Compared with published extraction methods, the proposed method is novel in the following aspects.

(1) The newly proposed IGBT modeling method is used to derive a new excess lifetime extraction theory.

(2) The 2D Sentaurus numerical simulation is performed to validate the proposed method. In the validation, the actual excess carrier lifetime of the 2D numerical device model is obtained. The proposed method is then directly verified by the comparison of the extracted and actual lifetime.

In the end, the good agreement between the actual carrier lifetime and the extracted value demonstrates the accuracy of the proposed extraction method.

REFERENCES

[1] A. T. Bryant, L. Lu, E. Santi, J. L. Hudgins, and P. R. Palmer, "Modeling of IGBT resistive and inductive turn-on behavior," *IEEE Trans. Ind. Appl.*, Vol. 44, No. 3, pp. 904-914, May/Jun. 2008.

[2] L. Lu, A. Bryant, J. L. Hudgins, P. R. Palmer, and E. Santi, "Physics-based model of planar-gate IGBT including MOS side two-dimensional effects," *IEEE Trans. Ind. Appl.*, Vol. 46, No.6, pp. 2556-2567, Nov./Dec. 2010.

[3] L. Lu, Z. Chen, A. Bryant, J. L. Hudgins, P. R. Palmer, and E. Santi, "Modeling of MOS-side carrier injection in trench-gate IGBTs," *IEEE Trans. Ind. Appl.*, Vol. 46, No. 2, pp. 875-883, Mar. 2010.

[4] S. Ryu, M. Lee, M. A. Hajji, H. Ahn, D. Han, and M. E. Nokali, "A transient model for insulated gate bipolar transistors (IGBTs)," *International Journal of Electronics*, Vol. 95, No. 4, pp. 399-409, Apr. 2008.

[5] Y. Tang, B. Wang, M. Chen, and B. Liu, "Simulation model and parameter extraction of field-stop(FS) IGBT," *Microelectronics Reliability*, Vol. 52, No. 12, pp. 2920-2931, Dec. 2012.

[6] X. Yang, M. Otsuki, and P. R. Palmer, "Physics-based insulated-gate bipolar transistor model with input capacitance correction," *IET Power Electronics*, Vol. 8, No. 3, pp. 417-427, Mar. 2015.

[7] A. R. Hefner and D. L. Blackburn, "An analytical model for the steady-state and transient characteristics of the power insulated-gate bipolar transistor," *Solid-State Electronics*, Vol. 31, No. 10, pp. 1513-1532, Oct. 1988.

[8] A. Hefner Jr, "Device models, circuit simulation, and computer-controlled measurements for the IGBT," in *IEEE Workshop on Comput. in Power Electron.*, pp. 233-243, 1990.

[9] X. Kang, E. Santi, J. L. Hudgins, P. R. Palmer, and J. Donlon, "Parameter extraction for a physics-based circuit simulator IGBT model," in *18th Annual IEEE Applied Power Electronics Conference and Exposition*, Vol. 2, pp. 946-952, Feb. 2003.

[10] A. Claudio, M. Cotorogea, and M. A. Rodriguez, "Parameter extraction for physics-based IGBT models by electrical measurements," in *IEEE 33rd Annual Power Electronics Specialists Conference*, Vol. 3, pp. 1295-1300, 2002.

[11] M. Cotorogea, A. Claudio, and M. Rodriguez, "Parameter extraction method for the pspice model of the PT-and NPT-IGBT's by electrical measurements," in *IEEE International Power Electronics Congress Technical Proceedings(CIEP)*, pp. 101-106, Oct. 2002.

[12] M. A. Rodrguez, A. Claudio, M. Cotorogea, L. H. Gonzlez, and J. Aguayo, "Reconfigurable special test circuit of physics-based IGBT models parameter extraction," *Solid-State Electronics*, Vol. 54, No. 11, pp. 1246-1256, Nov. 2010.

[13] Y. Tang, M. Chen, and B. Wang, "An improved method for IGBT base excess carrier lifetime extraction," in *International Conference on Applied Superconductivity and Electromagnetic Devices*, pp. 206-210, Sep. 2009.

[14] R.Withanage, N. Shammas, S.Tennakoorr, C. Oates, and W. Crookes, "IGBT parameter extraction for the hefner IGBT model," in *Proceedings of the 41st International Universities Power Engineering Conference*, Vol. 2, pp. 613-617, Sep. 2006.
[15] J. Karlsson, "The concept of IGBT modeling and the evaluation of the PSPICE IGBT model," *Master Thesis, Conducted at ALSTOM Power*, Växjö, 2002.
[16] Y. Tang, M. Chen, and B. Wang, "New methods for extracting Field-Stop IGBT model parameters by electrical measurements," in *IEEE International Symposium on Industrial Electronics(ISIE)*, pp. 1546-1551, Jul. 2009.
[17] A. R. Hefner, "Modeling buffer layer IGBTs for circuit simulation," *IEEE Trans. Power Electron.*, Vol. 10, No. 2, pp. 111-123, Mar. 1995.
[18] A. T. Bryant, X. Kang, E. Santi, P. R. Palmer, and J. L. Hudgins, "Two-step parameter extraction procedure with formal optimization for physics-based circuit simulator IGBT and pin diode models," *IEEE Trans. Power Electron.*, Vol. 21, No. 2, pp. 295-309, Mar. 2006.
[19] R.F. M. Chibante, A. L. S. Arajo, and A. S. Carvalho, "A simple and efficient parameter extraction procedure for physics based IGBT models," in *11th International Power Electronics and Motion Control Conference*, 2004.
[20] A. R. Hefner and D. L. Blackburn, "A performance trade-off for the insulated gate bipolar transistor: buffer layer versus base lifetime reduction," *IEEE Trans. Power Electron.*, Vol. PE-2, No. 3, pp. 194-207, Jul. 1987.

Guicui Fu received her M.S. degree in Aircraft Engineering from Northwestern Polytechnical University, Xian, China, in 1993, and her Ph.D. degree in System Engineering from Beihang University, Beijing, China, in 2005. Since 1993, she has been with the Beihang University, where she is currently a Professor in the School of Reliability and System Engineering. She has published over 40 technical papers and 4 books. Her research interests include thermal design and optimization, reliability engineering, and failure analysis of semiconductor devices.

Peng Xue is currently working toward his Ph.D. degree in the Beihang University, Beijing, China. His research interests include physical characterization and thermal modeling of power semiconductor devices, power electronics reliability, and conditional monitoring.